Estimation of semileptonic decays of B_c meson to S-wave charmonia with nonrelativistic QCD

Cong-Feng Qiao[1,2,*] and Rui-Lin Zhu[1,†]

[1]*Department of Physics, University of the Chinese Academy of Sciences, YuQuan Road 19A, Beijing 100049, China*
[2]*Kavli Institute for Theoretical Physics China, The Chinese Academy of Sciences, Beijing 100190, China*

(Received 31 August 2012; revised manuscript received 5 December 2012; published 8 January 2013)

We study the semileptonic differential decay rates of the B_c meson to S-wave charmonia, η_c, and J/Ψ at next-to-leading order accuracy in the framework of nonrelativistic QCD. In the heavy quark limit, $m_b \to \infty$, we obtain analytically the asymptotic expression for the ratio of the next-to-leading order form factor to the leading-order form factor. Numerical results show that the convergence of the ratio is perfect. At the maximum recoil region, we analyze the differential decay rates in detail with various input parameters and polarizations of J/ψ, which can now be checked in the LHCb experiment. Phenomenologically, the form factors are extrapolated to the minimal recoil region, and then the B_c-to-charmonium semileptonic decay rates are estimated.

DOI: 10.1103/PhysRevD.87.014009 PACS numbers: 12.38.Bx, 12.39.St, 13.20.−v

I. INTRODUCTION

The Large Hadron Collider (LHC) provides a large amount of data on B_c events, wherein the most easily identified decay modes to tag the B_c are the fully reconstructed channel $B_c \to J/\Psi\pi$ and the semileptonic decay channel $B_c \to J/\Psi\ell\nu(\ell = e, \mu)$. The CDF Collaboration made the first observation of the B_c meson by its semileptonic decay at the Tevatron fourteen years ago [1]. Later, the D0 Collaboration performed the same analysis in a sample of 210 pb^{-1} of the Run II data [2]. The cross section of B_c production at the LHC is larger than that at the Tevatron by roughly an order of magnitude, which reaches 49.8 nb at the center-of-mass energy $\sqrt{s} = 14$ TeV [3,4]. This makes the experimental study of the differential branching fraction of the B_c meson's semileptonic decays to charmonium feasible. We can also obtain information about the Cabibbo-Kobayashi-Maskawa matrix element in B_c decays, especially V_{cb}, which is not well-determined.

Recently, the *BABAR* collaboration measured the partial branching fraction $\Delta B/\Delta q^2$ in bins of the momentum-transfer squared, with $6q^2$ bins for $B^0 \to \pi^-\ell^+\nu$ and $3q^2$ bins for $B^0 \to \rho^-\ell^+\nu$ [5]. They found that the partial branching fraction of $B^0 \to \pi^-\ell^+\nu$ decreases as q^2 increases, while for the $B^0 \to \rho^-\ell^+\nu$ process the partial branching fraction first increases and then decreases as q^2 increases. Actually, we know that all five of the form factors in the above two decay channels at the maximum recoil region increases with q^2, at the next-to-leading order (NLO) accuracy according to the light-cone sum rules calculation [6,7]. The decrease of $B^0 \to \pi^-\ell^+\nu$ is caused by the phase space, which counteracts the enhancement from form factors. In this work, we try to determine whether this happens in B_c semileptonic decays to charmonia.

There exist several approaches in the calculation of B_c meson semileptonic decays to charmonium. These approaches include: the light-cone QCD sum rules (QCD LCSR) [8–11], the relativistic quark model [12,13], the instantaneous nonrelativistic approach to the Bethe-Salpeter equation [14], the nonrelativistic constituent quark model [15], the covariant light-front model [16], and the QCD potential model [17].

Considering that the B_c meson consists of two heavy quarks with different flavors—whose masses are much larger than the $\Lambda_{\rm QCD}$, analogous to the situation of heavy quarkonium—the system turns out to be nonrelativistic. Hence the relative velocity of heavy quarks within the B_c meson is small, i.e., $v \ll 1$, although it is bigger than the velocities of quarks in charmonium and bottomonium systems, and hence the nonrelativistic QCD (NRQCD) formalism is applicable to the study of B_c meson semileptonic decays to charmonia. In the NRQCD framework, the matrix elements of the concerned processes can be factorized as

$$\langle J/\psi(\eta_c)\ell\nu|\bar{c}\Gamma_\mu b\bar{l}\Gamma^\mu\nu|B_c\rangle \simeq \sum_{n=0}\psi(0)_{B_c}\psi(0)_{J/\psi(\eta_c)}T^n. \tag{1}$$

Here, $\Gamma^\mu = \gamma^\mu(1-\gamma_5)$, and the nonperturbative parameters $\psi(0)_{\bar{B}_c}$ and $\psi(0)_{J/\psi(\eta_c)}$ are the Schrödinger wave functions at the origin for $b\bar{c}$ and $c\bar{c}$ systems, respectively. T^n are hard scattering kernels which can be calculated perturbatively.

The paper is organized as follows. In Sec. II we present the definition for the relevant form factors and work out the expressions of the form factors in the NRQCD framework. In Sec. III the dependence of the NLO semileptonic differential decay rates on q^2 is obtained. In Sec. IV we calculate the decay width and study the theoretical uncertainty, and analyze the result in detail in the maximum recoil region. The last section is reserved for conclusions.

*qiaocf@gucas.ac.cn
†zhuruilin09@mails.gucas.ac.cn

II. FORM FACTORS

The $B_c \to J/\psi(\eta_c)$ transition form factors, f_+, f_0, V, A_0, A_1, and A_2 are normally defined as follows [18]:

$$\langle \eta_c(p)|\bar{c}\gamma^\mu b|B_c(P)\rangle = f_+(q^2)\left(P^\mu + p^\mu - \frac{m_{B_c}^2 - m_{\eta_c}^2}{q^2}q^\mu\right) + f_0(q^2)\frac{m_{B_c}^2 - m_{\eta_c}^2}{q^2}q^\mu, \tag{2}$$

$$\begin{aligned}\langle J/\psi(p,\varepsilon^*)|\bar{c}\gamma^\mu b|B_c(P)\rangle &= \frac{2iV(q^2)}{m_{B_c}+m_{J/\psi}}\epsilon^{\mu\nu\rho\sigma}\varepsilon_\nu^* p_\rho P_\sigma,\\ \langle J/\psi(p,\varepsilon^*)|\bar{c}\gamma^\mu\gamma_5 b|B_c(P)\rangle &= 2m_{J/\psi}A_0(q^2)\frac{\varepsilon^*\cdot q}{q^2}q^\mu - A_2(q^2)\frac{\varepsilon^*\cdot q}{m_{B_c}+m_{J/\psi}}\left(P^\mu + p^\mu - \frac{m_{B_c}^2 - m_{J/\psi}^2}{q^2}q^\mu\right)\\ &\quad + (m_{B_c}+m_{J/\psi})A_1(q^2)\left(\varepsilon^{*\mu} - \frac{\varepsilon^*\cdot q}{q^2}q^\mu\right).\end{aligned} \tag{3}$$

Here we define the momentum transfer $q = P - p$.

It is straightforward to calculate those form factors at the tree level in the NRQCD. They read

$$V^{\rm LO}(q^2) = \frac{16\sqrt{2}C_A C_F\pi(3z+1)\alpha_s\psi(0)_{B_c}\psi(0)_{J/\Psi}}{\left((1-z)^2 - \frac{q^2}{m_b^2}\right)^2\left(\frac{z}{z+1}\right)^{3/2}m_b^3 N_c}, \tag{4}$$

$$A_0^{\rm LO}(q^2) = \frac{16\sqrt{2}C_A C_F\pi(z+1)^{5/2}\alpha_s\psi(0)_{B_c}\psi(0)_{J/\Psi}}{\left((1-z)^2 - \frac{q^2}{m_b^2}\right)^2 z^{3/2}m_b^3 N_c}, \tag{5}$$

$$A_1^{\rm LO}(q^2) = \frac{16\sqrt{2}C_A C_F\pi\sqrt{z+1}(4z^3+5z^2+6z - \frac{q^2}{m_b^2}(2z+1)+1)\alpha_s\psi(0)_{B_c}\psi(0)_{J/\Psi}}{\left((1-z)^2 - \frac{q^2}{m_b^2}\right)^2 z^{3/2}(3z+1)m_b^3 N_c}, \tag{6}$$

$$A_2^{\rm LO}(q^2) = \frac{16\sqrt{2}C_A C_F\pi\sqrt{z+1}(3z+1)\alpha_s\psi(0)_{B_c}\psi(0)_{J/\Psi}}{\left((1-z)^2 - \frac{q^2}{m_b^2}\right)^2 z^{3/2}m_b^3 N_c}, \tag{7}$$

$$f_+^{\rm LO}(q^2) = \frac{8\sqrt{2}C_A C_F\pi\sqrt{z+1}\left(-\frac{q^2}{m_b^2}+3z^2+2z+3\right)\alpha_s\psi(0)_{B_c}\psi(0)_{\eta_c}}{\left((1-z)^2 - \frac{q^2}{m_b^2}\right)^2 z^{3/2}m_b^3 N_c}, \tag{8}$$

$$f_0^{\rm LO}(q^2) = \frac{8\sqrt{2}C_A C_F\pi\sqrt{z+1}(9z^3+9z^2+11z - \frac{q^2}{m_b^2}(5z+3)+3)\alpha_s\psi(0)_{B_c}\psi(0)_{\eta_c}}{\left((1-z)^2 - \frac{q^2}{m_b^2}\right)^2 z^{3/2}(3z+1)m_b^3 N_c}, \tag{9}$$

where $z \equiv m_c/m_b$.

There are three typical scales of the process, each of which possess the hierarchy of $\Lambda_{\rm QCD} \ll m_c \ll m_b$. Note that in Refs. [19–21], the form factors of B_c transition to η_c or J/Ψ with alternative parametrizations that have been calculated at NLO accuracy in the nonrelativistic limit. We expand the ratios of the NLO form factors to the leading-order (LO) form factors at first order in the $z = m_c/m_b$ expansion in the heavy quark limit $m_b \to \infty$. The asymptotic expressions of these form factors are then obtained analytically; the analysis can be found in the Appendix.

In the heavy quark limit, the form factors become

$$V(q^2)^{\rm LO}_{m_b\to\infty} = \frac{16\sqrt{2}C_A C_F\pi\alpha_s\psi(0)_{B_c}\psi(0)_{J/\Psi}}{\left(1 - \frac{q^2}{m_b^2}\right)^2 z^{3/2}m_b^3 N_c}, \tag{10}$$

$$A_2(q^2)_{m_b\to\infty} = V(q^2)_{m_b\to\infty}, \tag{11}$$

$$A_0(q^2)^{\rm LO}_{m_b\to\infty} = V(q^2)^{\rm LO}_{m_b\to\infty}, \tag{12}$$

$$A_1(q^2)_{m_b\to\infty} = \left(1-\frac{q^2}{m_b^2}\right)V(q^2)_{m_b\to\infty}, \tag{13}$$

$$f_+^{\rm LO}(q^2)_{m_b\to\infty} = \frac{\left(3-\frac{q^2}{m_b^2}\right)\psi(0)_{\eta_c}}{2\psi(0)_{J/\Psi}}V(q^2)^{\rm LO}_{m_b\to\infty}, \tag{14}$$

$$f_0^{\rm LO}(q^2)_{m_b\to\infty} = \frac{3\left(1-\frac{q^2}{m_b^2}\right)}{\left(3-\frac{q^2}{m_b^2}\right)}f_+^{\rm LO}(q^2)_{m_b\to\infty}. \tag{15}$$

At the $q^2=0$ point, some form factors turn out to be identical, namely,

$$f_0(0) = f_+(0), \tag{16}$$

$$V(0)_{m_b\to\infty} = A_1(0)_{m_b\to\infty} = A_2(0)_{m_b\to\infty}, \tag{17}$$

which are consistent with the heavy-quark effective theory [22] and the large-energy effective theory [23] predictions. Note that the equality (16) still holds beyond the heavy limit.

While approaching the minimal recoil region, the charmonium will keep still in the rest frame of the initial particle, while the invariant mass of the lepton and neutrino pair will turn to its maximum value. In this case, the gluon exchanged inside the hadrons becomes soft, which may result in an infinity in the evaluation.

There exist in the literature several different approaches for extrapolating the form factors to the minimal recoil region. One of these is the pole-mass dependence model developed in Refs. [16,24,25], where the form factors are parametrized as

$$f'(q^2) = \frac{f(0)}{1-q^2/m_{\rm pole}^2-\beta q^4/m_{\rm pole}^4}. \tag{18}$$

Here, β is a free parameter, which is set to zero in our calculation, (as was done in Ref. [24]), $m_{\rm pole}$ denotes the gluon effective pole mass, and $f'(q^2)$ represents any one of the form factors. In the latter calculation for decay widths, we will adopt this form. To regulate the infrared divergence induced by the soft gluon, one asks that the form factors $f'(q^2)$ satisfy the conditions

$$f'(q^2)_{q^2\to 0} = f(0), \qquad f'(q^2)_{q^2\to q^2_{\rm max}} = \text{constant}. \tag{19}$$

Here the constant represents the value of the form factors at the minimal recoil point and may be determined through a certain model. For example, we can parametrize the form factors as

$$f'(q^2) = f\left(\frac{q^2}{\sqrt{1+(q^2/q^2_{\rm cut})^2}}\right)e^{-S(q^2)}, \tag{20}$$

which satisfies $f'(q^2)\simeq f(q^2)$ in the maximum recoil region while becoming finite at the minimal recoil point. Here, the $S(q^2)$ meets the condition $S(0)=0$ and hence can be further parametrized as $S(q^2)=c_0q^2$, with c_0 a constant. $q^2_{\rm cut}$ is introduced to regularize the unphysical behavior of the form factors in the minimal recoil region. Note that the parameters $q^2_{\rm cut}$ and c_0 should either be determined through the phenomenological model or fitted by experimental data.

III. SEMILEPTONIC DIFFERENTIAL DECAY WIDTHS

For light leptons e and μ, their masses m_ℓ can be readily neglected; hence, the semileptonic differential decay rate of $B_c\to\eta_c\ell\nu$ depending on q^2 reads

$$\frac{d\Gamma}{dq^2}(B_c\to\eta_c\ell\nu) = \frac{G_F^2|V_{cb}|^2}{192\pi^3m_{B_c}^3}\lambda(q^2)^{3/2}[f_+(q^2)]^2. \tag{21}$$

Here, G_F is the Fermi constant, V_{cb} is the Cabibbo-Kobayashi-Maskawa matrix element, and $\lambda(q^2)=(m_{B_c}^2+m_{\eta_c}^2-q^2)^2-4m_{B_c}^2m_{\eta_c}^2$. The mass of the lepton τ cannot be ignored in the analysis, as it involves the form factors f_0 and f_+. However, f_0 can be measured via the $B_c\to\eta_c\tau\nu_\tau$ process, while f_+ can be obtained through $B_c\to\eta_c\ell\nu_\ell$ decay.

By virtue of the NLO form factors, we can easily gain the distribution of the NLO differential decay rate on momentum transfer q^2. To check the convergence behavior of the ratio of the NLO differential decay rate to the LO one, we select three sets of different values of z and scale q^2, as given in Table I, and we illustrate the parameter dependence in Figs. 1 and 2. Here, the Schrödinger wave function at the origin for J/Ψ is determined through its leptonic decay widths at the NLO level.

For the $B_c\to\eta_c\ell\nu$ channel, at the maximum recoil point $q^2=0$ we obtain a value of $4.67^{+0.38}_{-0.58}\times 10^{-12}|V_{cb}|^2$ GeV^{-1} for Eq. (21), which is larger than the value of $2.05\times10^{-12}|V_{cb}|^2$ GeV^{-1} obtained in QCD LCSR [11] and the value of $0.65\times10^{-12}|V_{cb}|^2$ GeV^{-1} obtained in the nonrelativistic quark model [15]. Besides,

TABLE I. Theoretical parameters for different sets, with renormalization scale $\mu=4.8$ GeV, the lifetime of the B_c $\tau(B_c)=0.453$ ps, and $G_F=1.16637\times10^{-5}$ GeV^{-2} [26], where m_b, m_c, and Λ are in units of GeV, while the $|\psi(0)|$'s are in units of GeV$^{3/2}$ [27,28].

	m_b	m_c	Λ	$\lvert\psi(0)\rvert_{B_c}$	$\lvert\psi(0)\rvert_{\eta_c}$	$\lvert\psi(0)\rvert_{J/\Psi}$
Set 1	4.8	1.5				
Set 2	4.9	1.4	0.10	0.3615	0.283	0.283
Set 3	5.0	1.3				

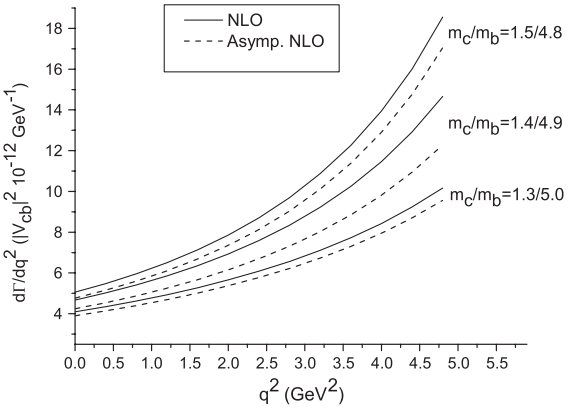

FIG. 1. NLO differential decay rate for the $B_c \to \eta_c \ell \nu$, for different values of the quark mass. The renormalization scale is chosen to be close to the bottom-quark mass, i.e., $\mu = 4.8$ GeV. In the figure, Asymp. NLO means expanding the ratio of the NLO form factor to the LO one at the first order in the $z = m_c/m_b$ expansion and in the heavy quark limit $m_b \to \infty$.

the results away from the maximum recoil point tend to disagree with those in Ref. [15]. In the NRQCD calculation, the form factors of B_c to η_c are obviously enhancing with an increase in q^2-despite the results from light-cone sum rules and nonrelativistic quark model—and the trend is sharpening at NLO, which counteracts the decrescence due to the phase space factor.

For the channel of $B_c \to J/\Psi \ell \nu (\ell = e, \mu)$, the decay rates in the transverse and longitudinal polarization of the vector meson J/Ψ can be formulated as

$$\frac{d\Gamma_L}{dq^2} = \frac{G_F^2 \lambda(q^2)^{1/2} |V_{cb}|^2 q^2}{192\pi^3 m_{B_c}^3} |H_0(q^2)|^2, \tag{22}$$

$$\frac{d\Gamma_T}{dq^2} = \frac{G_F^2 \lambda(q^2)^{1/2} |V_{cb}|^2 q^2}{192\pi^3 m_{B_c}^3} (|H_+(q^2)|^2 + |H_-(q^2)|^2), \tag{23}$$

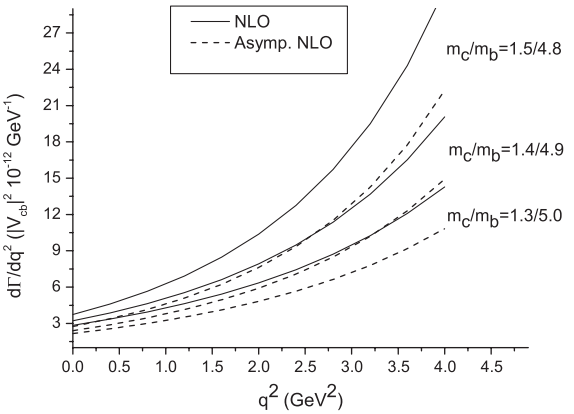

FIG. 2. NLO differential decay rate for $B_c \to J/\Psi \ell \nu$, for different values of the quark mass. The renormalization scale is chosen as $\mu = 4.8$ GeV.

respectively. Here the helicity amplitudes are expressed as follows:

$$H_\pm(q^2) = \frac{\lambda(q^2)^{1/2}}{m_{B_c} + m_{J/\Psi}} \left[V(q^2) \mp \frac{(m_{B_c} + m_{J/\Psi})^2}{\lambda(q^2)^{1/2}} A_1(q^2) \right], \tag{24}$$

$$H_0(q^2) = \frac{1}{2m_{J/\Psi}\sqrt{q^2}} \left[-\frac{\lambda(q^2)}{m_{B_c} + m_{J/\Psi}} A_2(q^2) + (m_{B_c} + m_{J/\Psi})(m_{B_c}^2 - m_{J/\Psi}^2 - q^2) A_1(q^2) \right]. \tag{25}$$

While summing up the various polarizations, the semileptonic differential decay rate of $B_c \to J/\Psi \ell \nu$ over q^2 is obtained:

$$\frac{d\Gamma}{dq^2}(B_c \to J/\Psi \ell \nu) = \frac{G_F^2 \lambda(q^2)^{1/2} |V_{cb}|^2 q^2}{192\pi^3 m_{B_c}^3} (|H_+(q^2)|^2 + |H_-(q^2)|^2 + |H_0(q^2)|^2), \tag{26}$$

with $\lambda(q^2) = (m_{B_c}^2 + m_{J/\Psi}^2 - q^2)^2 - 4m_{B_c}^2 m_{J/\Psi}^2$.

Similarly to $B_c \to \eta_c \ell \nu$, the distribution of the NLO differential decay rate on momentum transfer q^2 for the $B_c \to J/\Psi \ell \nu$ channel with three sets of different values of z is illustrated in Fig. 2. At the maximum recoil point $q^2 = 0$, we obtain a value of $3.21^{+0.53}_{-0.37} \times 10^{-12} |V_{cb}|^2\,\mathrm{GeV}^{-1}$ for Eq. (26), which is larger than the value of $0.6 \times 10^{-12} |V_{cb}|^2\ \mathrm{GeV}^{-1}$ obtained in the nonrelativistic quark model [15]. Except for the enhancement from the NLO K-factor and the NLO Schrödinger wave functions at the origin, the result in LO in the NRQCD calculation is intrinsically bigger than that obtained in the nonrelativistic quark model.

IV. THEORETICAL UNCERTAINTY

With the input parameters given in Table I and taking $m_{B_c} = 6.273$ GeV [29], one can readily obtain the decay widths numerically, which are presented in Table II. In our calculation, the value of the J/Ψ wave function squared at the origin is extracted from the leptonic decay width at NLO in α_s [33,34], i.e.,

$$|\psi(0)|^2_{J/\Psi} = \frac{m_{J/\Psi}^2}{16\pi\alpha^2 e_c^2} \frac{\Gamma(J/\Psi \to e^+ e^-)}{(1 - 4\alpha_s C_F/\pi)}, \tag{27}$$

and the experimental value $\Gamma(J/\Psi \to e^+ e^-) = 5.55 \pm 0.14 \pm 0.02$ keV is used. Note that according to the heavy-quark spin symmetry, at leading order in the typical velocity v expansion in NRQCD we have $|\psi(0)|_{\eta_c} = |\psi(0)|_{J/\Psi}$.

It is found that the main uncertainties of the concerned processes come from two sources: the heavy quark masses

TABLE II. The branching ratios (in %) of exclusive semileptonic decays of the B_c meson to ground-state charmonia, in comparison with the results of light-cone sum rules [11,24], the quark model [13,15,16,25,30], the calculation of the Bethe-Salpeter equation [14], and the QCD relativistic potential model [31,32]. In the evaluation, the B_c lifetime $\tau(B_c) = 0.453$ ps, ℓ stands for e or μ, $m_c/m_b = 1.4/4.9$, $\mu = 4.8$ GeV, and $|V_{cb}| = 0.0406$. The uncertainties in our calculation come from varying the value of m_c/m_b from 1.5/4.8 to 1.3/5.0, varying the renormalization scale μ from 3 to 6 GeV, and varying the pole mass $m_{\rm pole}$ from 4.25 to 4.75 GeV^2 [8,24], respectively.

Mode	This paper	[8,24]	[11]	[15]	[16]	[25]	[30]	[13]	[14]	[31]	[32]
$B_c^- \to \eta_c \ell \nu$	$2.1^{+0.5+0.4+0.2}_{-0.3-0.1-0.1}$	0.75	1.64	0.48	0.67	0.59	0.81	0.40	0.97	0.15	0.76
$B_c^- \to \eta_c \tau \nu$	$0.64^{+0.07+0.14+0.10}_{-0.08-0.06-0.05}$	0.23	0.49	0.16	0.19	0.20	0.22	...	...	...	...
$B_c^- \to J/\psi \ell \nu$	$6.7^{+2.1+1.0+0.9}_{-1.2-0.4-0.6}$	1.9	2.37	1.5	1.49	1.20	2.07	1.21	2.35	1.47	2.01
$B_c^- \to J/\psi \tau \nu$	$0.52^{+0.16+0.08+0.08}_{-0.09-0.03-0.05}$	0.48	0.65	0.4	0.37	0.34	0.49	...	...	...	...

TABLE III. The NLO partial decay widths for various q^2. For J/Ψ, the partial decay widths for transverse ($\varepsilon_\perp^*$) and longitudinal ($\varepsilon_\parallel^*$) polarizations are presented separately.

Bins of q^2 (GeV^2)	$0 \le q^2 \le 1$	$1 \le q^2 \le 2$	$2 \le q^2 \le 3$	$3 \le q^2 \le 4$	$4 \le q^2 \le 5$
$\Delta\Gamma(B_c \to \eta_c \ell \nu)(10^{-15}$ GeV)	$8.06^{+1.17+1.96}_{-0.77-0.74}$	$9.73^{+1.78+2.37}_{-1.16-0.89}$	$12.0^{+2.78+2.95}_{-1.77-1.11}$	$15.2^{+4.47+2.73}_{-3.77-1.41}$	$20.0^{+7.57+5.06}_{-4.36-1.87}$
$\Delta\Gamma(B_c \to J/\Psi(\varepsilon_\perp^*) \ell \nu)(10^{-15}$ GeV)	$0.70^{+0.215+0.159}_{-0.141-0.061}$	$2.64^{+0.95+0.60}_{-0.60-0.23}$	$5.84^{+2.54+1.34}_{-1.51-0.51}$	$11.28^{+6.03+2.61}_{-3.35-1.00}$	$20.97^{+14.14+4.90}_{-7.16-1.87}$
$\Delta\Gamma(B_c \to J/\Psi(\varepsilon_\parallel^*) \ell \nu)(10^{-15}$ GeV)	$6.01^{+1.14+1.40}_{-0.78-0.53}$	$7.87^{+1.93+1.84}_{-1.27-0.70}$	$10.64^{+3.38+2.51}_{-2.72-0.95}$	$14.96^{+6.18+3.56}_{-3.62-1.35}$	$22.07^{+12.06+5.31}_{-6.45-2.01}$
$\Delta\Gamma(B_c \to J/\Psi \ell \nu)(10^{-15}$ GeV)	$6.71^{+1.35+1.56}_{-0.92-0.59}$	$10.52^{+2.89+2.45}_{-1.88-0.93}$	$16.49^{+5.92+3.86}_{-4.24-1.47}$	$26.24^{+12.21+6.18}_{-6.98-2.35}$	$43.04^{+26.20+10.22}_{-13.61-3.88}$

TABLE IV. The NLO partial decay widths of the processes $B_c \to \eta_c \tau \nu_\tau$ and $B_c \to J/\Psi \tau \nu_\tau$ for various q^2, where the maximum recoil point is at m_τ^2.

Bins of q^2 (GeV^2)	$m_\tau^2 \le q^2 \le 4$	$4 \le q^2 \le 5$
$\Delta\Gamma(B_c \to \eta_c \tau \nu_\tau)(10^{-15}$ GeV)	$2.460^{+0.9245+0.655}_{-0.538-0.241}$	$17.62^{+8.42+4.70}_{-4.56-1.73}$
$\Delta\Gamma(B_c \to J/\Psi \tau \nu_\tau)(10^{-15}$ GeV)	$0.821^{+0.375+0.194}_{-0.213-0.073}$	$6.922^{+4.017+1.648}_{-2.107-0.625}$

and the renormalization scale. In the evaluation, we vary the charm-quark mass $m_c = 1.4$ GeV by ± 0.1 GeV, the bottom-quark mass $m_b = 4.9$ GeV by ± 0.1 GeV, and the renormalization scale $\mu = 4.8$ GeV by $^{+1.2}_{-1.8}$ GeV. The numerical value of the pole mass may vary in a reasonable range, so we also need to consider the uncertainty coming from the pole mass. Notice that the pole-mass effect tends to be small in the maximum recoil region, as it should be.

In Table II, the decay widths calculated through other approaches—such as QCD light-cone sum rules, the quark model, the Bethe-Salpeter equation, and the potential model—are also given. In comparison with the QCD LCSR results, our results are almost treble of theirs. This is understandable considering the large QCD correction K-factor and the NLO charmonium wave function employed.

To see more clearly the uncertainty remaining in the NLO evaluation, we calculate the decay width in various momentum transfer squared regions. For light leptons ($\ell = e$, μ), we divide q^2 into five bins in the maximum recoil region ($0 \le q^2 \le 5$ GeV^2) and calculate the semileptonic decay rates separately. The results are presented in Table III. We find that at small q^2 ($0 \le q^2 \le 1$ GeV^2), the longitudinally polarized J/Ψ events dominate over the transversally polarized ones by a factor of 8.5, and the difference reduces with an increase in q^2. For the lepton τ, we divide q^2 into two bins ($m_\tau^2 \le q^2 \le 4$, $4 \le q^2 \le 5$ GeV^2) in the maximum recoil region. Here the physical mass of the lepton τ is taken to be $m_\tau = 1.776$ GeV [26], and the results are shown in Table IV.

V. CONCLUSIONS

The NLO semileptonic differential decay rates of the B_c meson to charmomia were analyzed in detail with various choices of parameters. The uncertainties of the patrial decay widths in different bins of momentum transfer q^2 were evaluated. For the $B_c \to J/\Psi \ell \nu$ process, the partial decay widths for transverse and longitudinal polarizations were investigated separately. The distribution in the maximum recoil is found testable in the LHCb experiment, and in turn the NRQCD factorization will also be testable. Based on this particular model, the form factors were phenomenologically extrapolated to the minimal recoil region, and we estimated the total rates of B_c semileptonic decay to charmonium.

ACKNOWLEDGMENTS

This work was supported in part by the National Natural Science Foundation of China (NSFC) under the Grants No. 10935012, No. 10821063, and No. 11175249.

APPENDIX: THE NLO B_c-TO-CHARMONIA TRANSITION FORM FACTORS

In this appendix, the QCD NLO B_c-to-charmonium transition form factors are given at the first order in powers of m_c/m_b. For compactness, we define $z = m_c/m_b$, $s = \frac{m_b^2}{m_b^2 - q^2}$, and $\gamma = \frac{m_b^2 - q^2}{4 m_b m_c}$. The form factors at the maximum recoil point, i.e., $q^2 = 0$, are also presented, which are in agreement with those given in Refs. [19,21].

$$\begin{aligned}\frac{f_+^{\rm NLO}(q^2)}{f_+^{\rm LO}(q^2)} &= 1 + \frac{\alpha_s}{4\pi}\left\{\frac{1}{3}(11C_A - 2n_f)\log\left(\frac{\mu^2}{2\gamma m_c^2}\right) - \frac{10n_f}{9} + \frac{(\pi^2 - 6\log(2))(s-1) + 3s\log(\gamma)}{6s+3}\right.\\
&+ \frac{C_A}{72s^2-18}(18s^2(2s-1)\log^2(s) + 18(8\log(2)s^3 - 2\log(2)s^2 - 5\log(2)s + s + 2\log(2))\log(s)\\
&+ (2s-1)(268s + \pi^2(6s^2 - 3s - 6) + 170) - 9(2s-1)\log(\gamma)(\log(\gamma)s - (2 + 2\log(2))s + 4\log(2))\\
&+ 18(2s-1)(4s^2 + s - 2){\rm Li}_2(1-2s) - 18(4s^3 - 5s + 2){\rm Li}_2(1-s) + 18(s(4s(s+1) - 11) + 4)\log^2(2)\\
&- 36(5(s-1)s + 1)\log(2)) + \frac{C_F}{6(1-2s)^2(2s+1)}(-6(2(s-1)s - 1)\log^2(s)(1-2s)^2\\
&+ 3\log(\gamma)(23s + (5s-2)\log(\gamma) - 4(s+1)\log(2) + 12)(1-2s)^2 - 12(4s^2 + s - 2){\rm Li}_2(1-2s)(1-2s)^2\\
&+ 12(s(2s+3) - 1){\rm Li}_2(1-s)(1-2s)^2 - (\pi - 2\pi s)^2(s(4s - 19) + 4) + 3(-32\log^2(2)s^4\\
&- 4(69 + 2\log(2)(-37 + 5\log(2)))s^3 + 8(18 + \log(2)(-31 + 9\log(2)))s^2 + (61 + 28\log(2)\\
&- 26\log^2(2))s + 12\log(2) + 2\log^2(2) - 32) + (6s(8s(s(-4\log(2)s + 3\log(2) + 3) + 2\log(2) - 3)\\
&\left.- 18\log(2) + 7) + 24\log(2))\log(s))\right\}, \end{aligned} \tag{A1}$$

$$\begin{aligned}\frac{f_+^{\rm NLO}(0)}{f_+^{\rm LO}(0)} &= 1 + \frac{\alpha_s}{4\pi}\left\{\frac{1}{3}(11C_A - 2n_f)\log\left(\frac{2\mu^2}{m_b m_c}\right) - \frac{10n_f}{9} - \frac{1}{3}\log(z) - \frac{2\log(2)}{3}\right.\\
&+ C_F\left(\frac{1}{2}\log^2(z) + \frac{10}{3}\log(2)\log(z) - \frac{35}{6}\log(z) + \frac{2\log^2(2)}{3} + 3\log(2) + \frac{7\pi^2}{9} - \frac{103}{6}\right)\\
&\left.+ C_A\left(-\frac{1}{6}\log^2(z) - \frac{1}{3}\log(2)\log(z) - \frac{1}{3}\log(z) + \frac{\log^2(2)}{3} - \frac{4\log(2)}{3} - \frac{5\pi^2}{36} + \frac{73}{9}\right)\right\}, \end{aligned} \tag{A2}$$

$$\begin{aligned}\frac{f_0^{\rm NLO}(q^2)}{f_0^{\rm LO}(q^2)} &= 1 + \frac{\alpha_s}{4\pi}\left\{\frac{1}{3}(11C_A - 2n_f)\log\left(\frac{\mu^2}{2\gamma m_c^2}\right) - \frac{10n_f}{9} + \frac{\log(\gamma)}{3} + \frac{C_A}{36s-18}(-6{\rm Li}_2(1-s)(1-2s)^2\right.\\
&+ 6\log^2(2)(1-2s)^2 + 6s(2s-1)\log^2(s) + (2s-1)(\pi^2(2s-3) + 146) + (12s\log(2)(4s-3)\\
&+ 6\log(2) - 6)\log(s) - 3(2s-1)\log(\gamma)(\log(4\gamma) - 2) + 6(8s^2 - 6s + 1){\rm Li}_2(1-2s) - 12s\log(2))\\
&+ \frac{C_F}{18(1-2s)^2(s-1)}(-6(s-1)(2s-3)\log^2(s)(1-2s)^2 - 12(s-1)(4s-1){\rm Li}_2(1-2s)(1-2s)^2\\
&+ 24(s^2-1){\rm Li}_2(1-s)(1-2s)^2 - 6(-6s(2s(3s-8) + 11) + 2s(4s(s(4s-9) + 7) - 9)\log(2)\\
&+ 2\log(2) + 13)\log(s) + (s-1)(3\log(\gamma)(3\log(\gamma) - 8\log(2) + 35)(1-2s)^2 - 24(s+2)\log^2(2)(1-2s)^2\\
&\left.- (2s-1)(546s + \pi^2(8s^2 - 34s + 15) - 279) + 24(s(43s-42) + 10)\log(2)))\right\}, \end{aligned} \tag{A3}$$

$$\frac{f_0^{\rm NLO}(0)}{f_0^{\rm LO}(0)} = \frac{f_+^{\rm NLO}(0)}{f_+^{\rm LO}(0)}, \tag{A4}$$

$$\frac{V^{\mathrm{NLO}}(q^2)}{V^{\mathrm{LO}}(q^2)} = 1 + \frac{\alpha_s}{4\pi}\Big\{\frac{1}{3}(11C_A - 2\mathrm{n}_f)\log\Big(\frac{\mu^2}{2\gamma \mathrm{m}_c^2}\Big) - \frac{10\mathrm{n}_f}{9} - \frac{C_A}{36s-18}(9s(2s-1)\log^2(s)$$
$$+ 18(2s\log(2)(2s-1)+1)\log(s) + 3\pi^2(s+2)(2s-1) - 2s(-18\log^2(2)s + 9\log^2(2)$$
$$+ 45\log(2) + 134) + 9(2s-1)(\log(\gamma)-3)\log(\gamma) + 18s(2s-1)(2\mathrm{Li}_2(1-2s) - \mathrm{Li}_2(1-s))$$
$$+ 63\log(2) + 134) + \frac{C_F}{6(1-2s)^2(s-1)}(6(s^2-1)\log^2(s)(1-2s)^2 + 24(s-1)s\mathrm{Li}_2(1-2s)(1-2s)^2$$
$$+ 3(2s(s(4s(4\log(2)s - 8\log(2)+3) + 20\log(2) - 17) - 4\log(2) + 7) - 1)\log(s)$$
$$+ (s-1)(6\log(\gamma)(\log(\gamma) - 6\log(2) + 5)(1-2s)^2 + 6(2s-9)\log^2(2)(1-2s)^2$$
$$+ (2s-1)(-204s + 2\pi^2(2s^2+s-1) + 105) + 6(s(68s-67)+16)\log(2))$$
$$- 12(2s^2-3s+1)^2\mathrm{Li}_2(1-s))\Big\}, \tag{A5}$$

$$\frac{V^{\mathrm{NLO}}(0)}{V^{\mathrm{LO}}(0)} = 1 + \frac{\alpha_s}{4\pi}\Big\{\frac{1}{3}(11C_A - 2\mathrm{n}_f)\log\Big(\frac{2\mu^2}{m_b m_c}\Big) - \frac{10\mathrm{n}_f}{9}$$
$$+ C_F\Big(\log^2(z) + 10\log(2)\log(z) - 5\log(z) + 9\log^2(2) + 7\log(2) + \frac{\pi^2}{3} - 15\Big)$$
$$+ C_A\Big(-\frac{1}{2}\log^2(z) - 2\log(2)\log(z) - \frac{3}{2}\log(z) - 3\log^2(2) - \frac{3\log(2)}{2} - \frac{\pi^2}{3} + \frac{67}{9}\Big)\Big\}, \tag{A6}$$

$$\frac{A_1^{\mathrm{NLO}}(q^2)}{A_1^{\mathrm{LO}}(q^2)} = \frac{A_2^{\mathrm{NLO}}(q^2)}{A_2^{\mathrm{LO}}(q^2)} = \frac{V^{\mathrm{NLO}}(q^2)}{V^{\mathrm{LO}}(q^2)}, \tag{A7}$$

$$\frac{A_0^{\mathrm{NLO}}(q^2)}{A_0^{\mathrm{LO}}(q^2)} = 1 + \frac{\alpha_s}{4\pi}\Big\{\frac{1}{3}(11C_A - 2\mathrm{n}_f)\log\Big(\frac{\mu^2}{2\gamma \mathrm{m}_c^2}\Big) - \frac{10\mathrm{n}_f}{9} + \frac{C_A}{72(s-1)s(2s-1)}(-9(s-1)s(2s-1)(2s+1)\log^2(s)$$
$$- 9(2s(2s(\log(2)(4s^2-9)+3) + 12\log(2) - 3) - 4\log(2) - 2)\log(s)$$
$$+ (s-1)(-18(2s-1)\log^2(2)(s(2s+9)-4) - (2s-1)(s(3\pi^2(2s+9) - 608) + 36)$$
$$- 9(2s-1)\log(\gamma)(2\log(\gamma)s + 8\log(2)s - 6s + \log(\gamma) - 4\log(2) - 3) + 9(4s(13s-7) - 3)\log(2))$$
$$- 36(s(4s^3 - 9s + 6) - 1)\mathrm{Li}_2(1-2s) + 18(s-1)(2s-1)(s(2s+5)-2)\mathrm{Li}_2(1-s))$$
$$+ \frac{C_F}{24s(2s^2-3s+1)^2}(2\pi^2(1-2s)^2(s(2s-1)+3)(s-1)^2 + 24(1-2s)^2(s(2s+3)-1)\mathrm{Li}_2(1-2s)(s-1)^2$$
$$+ 6s(2s+5)(2s^2-3s+1)^2\log^2(s) + 3(s(s(2s\log(2)(2s(76s-193)+289)$$
$$+ 4s(-120s^2 + 369s + (8s^3 - 52s^2 + 90s - 43)\log^2(2) - 406) - 84\log^2(2) - 28\log(2) + 747)$$
$$+ 92\log^2(2) - 110\log(2) - 116) + 16\log^2(2) + 4(7 - 9\log(2))\log(2) - 3) + 3(s(2s(s(2s(4s(4\log(2)s$$
$$- 6\log(2) + 6) - 28\log(2) - 69) + 156\log(2) + 113) - 2(13 + 58\log(2))) + 72\log(2) - 5)$$
$$- 8\log(2) + 1)\log(s) - 6(2s^2-3s+1)^2(16\log(2)s - 22s - 2\log(\gamma) + 4\log(2) + 1)\log(\gamma)$$
$$- 12(2s^2-3s+1)^2(2s^2+s-2)\mathrm{Li}_2(1-s))\Big\}, \tag{A8}$$

$$\frac{A_0^{\mathrm{NLO}}(0)}{A_0^{\mathrm{LO}}(0)} = 1 + \frac{\alpha_s}{4\pi}\Big\{\frac{1}{3}(11C_A - 2\mathrm{n}_f)\log\Big(\frac{2\mu^2}{m_b m_c}\Big) - \frac{10\mathrm{n}_f}{9}$$
$$+ C_F\Big(\frac{1}{2}\log^2(z) - \frac{119}{8} + 7\log(2)\log(z) - \frac{21}{4}\log(z) + 7\log^2(2) + \frac{15\log(2)}{4}\Big)$$
$$+ C_A\Big(-\frac{3}{8}\log^2(z) - \log(2)\log(z) - \frac{9}{8}\log(z) - \frac{7\pi^2}{24} + \frac{67}{9} - \frac{9\log^2(2)}{4} + \frac{3\log(2)}{8}\Big)\Big\}. \tag{A9}$$

[1] F. Abe *et al.* (CDF Collaboration), Phys. Rev. Lett. **81**, 2432 (1998); Phys. Rev. D **58**, 112004 (1998).

[2] D. Lucchesi, in *ICHEP 2004*, edited by H. Chen *et al.* (World Scientific, Singapore, 2005), p. 158.

[3] N. Brambilla *et al.* (Quarkonium Working Group), Report No. CERN-2005-005.

[4] C.-H. Chang, C. Driouichi, P. Eerola, and X.-G. Wu, Comput. Phys. Commun. **159**, 192 (2004).

[5] P. del Amo Sanchez *et al.* (*BABAR* Collaboration), Phys. Rev. D **83**, 032007 (2011).

[6] P. Ball and R. Zwicky, Phys. Rev. D **71**, 014015 (2005).

[7] P. Ball and R. Zwicky, Phys. Rev. D **71**, 014029 (2005).

[8] V. V. Kiselev, A. E. Kovalsky, and A. K. Likhoded, Nucl. Phys. **B585**, 353 (2000).

[9] I. P. Gouz, V. V. Kiselev, A. K. Likhoded, V. I. Romanovsky, and O. P. Yushchenko, Yad. Fiz. **67**, 1581 (2004) [Phys. At. Nucl. **67**, 1559 (2004)].

[10] T. Huang and F. Zuo, Eur. Phys. J. C **51**, 833 (2007).

[11] T. Huang, Z.-H. Li, X.-G. Wu, and F. Zuo, Int. J. Mod. Phys. A **23**, 3237 (2008).

[12] M. A. Ivanov, J. G. Körner, and P. Santorelli, Phys. Rev. D **63**, 074010 (2001).

[13] D. Ebert, R. N. Faustov, and V. O. Galkin, Phys. Rev. D **68**, 094020 (2003).

[14] C. H. Chang and Y. Q. Chen, Phys. Rev. D **49**, 3399 (1994).

[15] E. Hernandez, J. Nieves, and J. M. Verde-Velasco, Phys. Rev. D **74**, 074008 (2006).

[16] W. Wang, Y. L. Shen, and C. D. Lü, Phys. Rev. D **79**, 054012 (2009).

[17] K. K. Pathak and D. K. Choudhury, arXiv:1109.4468.

[18] M. Wirbel, B. Stech, and M. Bauer, Z. Phys. C **29**, 637 (1985); M. Bauer, B. Stech, and M. Wirbel, Z. Phys. C **34**, 103 (1987).

[19] G. Bell, Ph.D. thesis, Ludwig Maximilian University of Munich, 2006, arXiv:0705.3133.

[20] G. Bell and T. Feldmann, Nucl. Phys. B, Proc. Suppl. **164**, 189 (2007).

[21] C.-F. Qiao, P. Sun, and F. Yuan, J. High Energy Phys. 08 (2012) 087.

[22] B. Stech, Phys. Lett. B **354**, 447 (1995); J. M. Soares, Phys. Rev. D **54**, 6837 (1996).

[23] J. Charles, A. Le Yaouanc, L. Oliver, O. Pène, and J. C. Raynal, Phys. Rev. D **60**, 014001 (1999).

[24] V. V. Kiselev, arXiv:hep-ph/0211021.

[25] A. Y. Anisimov, I. M. Narodetsky, C. Semay, and B. Silvestre-Brac, Phys. Lett. B **452**, 129 (1999); A. Y. Anisimov, P. Y. Kulikov, I. M. Narodetsky, and K. A. Ter-Martirosian, Yad. Fiz. **62**, 1868 (1999) [Phys. At. Nucl. **62**, 1739 (1999)].

[26] K. Nakamura *et al.* (Particle Data Group), J. Phys. G **37**, 075021 (2010).

[27] E. J. Eichten and C. Quigg, Phys. Rev. D **49**, 5845 (1994).

[28] C.-F. Qiao, L.-P. Sun, and R.-L. Zhu, J. High Energy Phys. 08 (2011) 131.

[29] R. Aaij *et al.* (LHCb Collaboration), Phys. Rev. Lett. **109**, 232001 (2012).

[30] M. A. Ivanov, J. G. Körner, and P. Santorelli, Phys. Rev. D **73**, 054024 (2006).

[31] P. Colangelo and F. De Fazio, Phys. Rev. D **61**, 034012 (2000).

[32] A. A. El-Hady, J. H. Munoz, and J. P. Vary, Phys. Rev. D **62**, 014019 (2000).

[33] G. T. Bodwin, E. Braaten, and G. P. Lepage, Phys. Rev. D **51**, 1125 (1995); **55**, 5853E (1997).

[34] Y.-J. Zhang and K.-T. Chao, Phys. Rev. Lett. **98**, 092003 (2007).